AJNR

Recurring patterns of inflammatory sinonasal disease demonstrated on screening sinus CT.

R W Babbel, H R Harnsberger, J Sonkens and S Hunt

This information is current as of September 2, 2025.

Recurring Patterns of Inflammatory Sinonasal Disease Demonstrated on Screening Sinus CT

Robert W. Babbel,[1] H. Ric Harnsberger,[1,3] Jerry Sonkens,[2] and Steven Hunt[1]

Purpose: In order to define specific features on screening sinus CT (SSCT) that will aid the endoscopic surgeon in his approach to patients with inflammatory sinonasal disease, we sought to answer four questions: 1) what recurring patterns of inflammatory sinonasal disease are evident on SSCT; 2) what is the relative frequency of these recurring patterns; 3) how do these CT patterns correlate with the known sinus mucociliary drainage routes; and 4) what are the characteristic radiologic features of each pattern? **Methods:** We reviewed the clinical and radiologic records of 500 consecutive patients who underwent SSCT as a prelude to possible functional endoscopic sinus surgery. **Results:** Five recurring radiologic patterns of sinonasal inflammatory disease were identified: 1) *infundibular* (129/500 or 26%), 2) *ostiomeatal unit* (126/500 or 25%) 3) *sphenoethmoidal recess* (32/500 or 6%), 4) *sinonasal polyposis* (49/500 or 10%), and 5) *sporadic* (*unclassifiable*) (121/500 or 24%) patterns. Normal SSCT was seen in 133/500 patients (27%). **Conclusion:** Identification of specific patterns of sinonasal disease permits grouping of patients into nonsurgical (normal CT), routine (infundibular, ostiomeatal unit, and most sporadic patterns) and complex (sinonasal polyposis and sphenoethmoidal recess patterns) surgical groups. Assignment of patients to radiologic patterns allows a tailored surgical approach.

Index terms: Paranasal sinuses, computed tomography; Paranasal sinuses, inflammation; Nose, computed tomography

Functional endoscopic sinonasal surgery (FESS) is widely utilized for the evaluation and treatment of inflammatory sinonasal disease (1–9). The use of this popular surgical procedure has resulted in a dramatic increase in the volume of radiologic studies obtained as part of presurgical evaluation of the paranasal sinuses. Computed tomography (CT) in the form of coronal screening sinus CT (SSCT) has emerged as the standard for preendoscopic assessment of the paranasal sinuses (3, 10–15). In this report we use the term SSCT to denote a limited preendoscopic sinus CT performed in a single plane without contrast and at a reduced cost (Table 1). It became evident during our routine interpretation of SSCT exams that there are recurring patterns of inflammatory sinonasal disease. To better understand these patterns, and in an attempt to render more useful SSCT reports to our referring clinicians, we reviewed 500 SSCT scans obtained over a 12-month period. Answers to four specific study questions were sought: 1) what recurring patterns of inflammatory sinonasal disease are evident on SSCT; 2) what is the relative frequency of these recurring patterns; 3) how do these CT patterns correlate with the known sinus mucociliary drainage routes; and 4) what are the characteristic radiologic features of each pattern?

FESS has been documented to be practical and successful in the therapeutic approach of patients with chronic inflammatory sinonasal disease (1, 2). The normal mucociliary drainage is dependent on patency of sinus ostia (3, 16–18). Messerklinger and others have shown that wherever there is contact of two opposing mucosal surfaces, normal mucociliary action is disrupted, allowing mucous and debris to accumulate, and thus creating increased potential for infection,

TABLE 1: Screening sinus CT technique protocol

Patient preparation

Key for eliminating reversible disease. Permits better delineation of anatomy and definition of chronic disease requiring endoscopic surgery. Includes:

1) completion of antibiotic course;

2) Continuation of oral antihistamines and decongestants;

3) Sympathomimetic nasal spray 15 minutes prior to exam, followed by vigorous nose blowing;

4) Consideration for steroids in allergic patients

CT technique

Patient position:

Prone coronal with head hyperextended, resting on chin (keeps free fluid out of infundibulum). In patients unable to maintain prone position or in cases where questions arise from prone images use supine coronal position with head hyperextended over edge of table

Gantry angle:

Perpendicular to hard palate to obtain direct coronal images; actual coronal angle is not critical

Scan extent:

Posterior margin of sphenoid sinus to anterior margin of frontal sinus

Section thickness:

Posterior 1/2 (posterior margin of sphenoid sinus to anterior margin of posterior ethmoid) done with 5-mm contiguous slices. Anterior 1/2 (anterior margin of posterior ethmoid to anterior margin of frontal sinus) done with 3-mm contiguous slices; the anterior thin sections are critical to insure optimal visualization of the OMU.

kVp: 120

mA (dose per slice):

200 (100 mA × 2 sec scan time) or less; low exposure can be used because of bone algorithm technique with filming at intermediate window

Imaging algorithm:

Bone (maximum edge enhancement program)

Photography:

Window width: 2000–2500 HU

Window center: 100–300 HU range

Both bone and soft tissues visualized on the single set of images.

Contrast: none

Note.—These recommendations are for screening sinus CT in evaluating inflammatory disease. In noninflammatory cases, or in extensive or complicated inflammatory cases, a full sinus CT should be considered. This includes intravenous contrast with axial and coronal imaging and with multiple filming techniques.
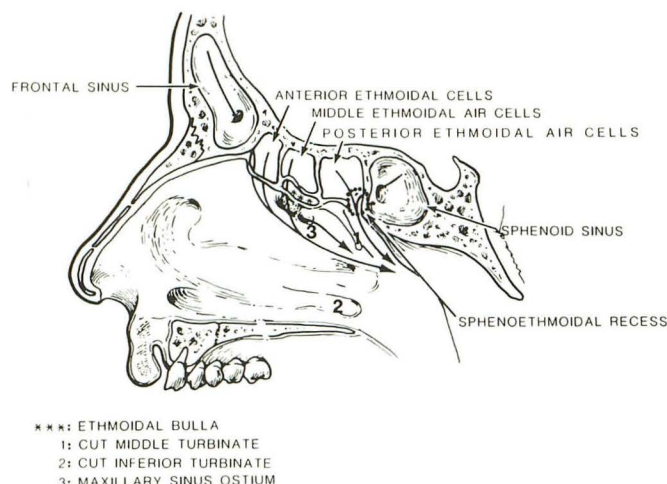

Fig. 1. Line drawing of lateral wall of nose depicting two main areas of mucociliary drainage. OMU region includes maxillary sinus ostium and ethmoidal bulla (draining anterior and middle ethmoid air cells) within hiatus semilunaris region. Nasofrontal duct drains into this region anteriorly. Disease within OMU results in *ostiomeatal unit pattern* of sinus disease. More posteriorly, sphenoid sinus drains posterior to superior turbinate while posterior ethmoid sinuses drain into superior meatus. This area is designated sphenoethmoidal recess (*dotted circle*) with obstruction in this area resulting in *sphenoethmoidal recess pattern* of inflammatory sinus disease.

even in the absence of ostial closure (16–18). Obstruction with associated dysfunction of mucociliary drainage is postulated to account for the majority of recurring inflammatory sinonasal disease (3, 12, 16–18). One of the main goals of FESS is to reestablish normal mucociliary drainage (3, 4, 6). It is probable that by identifying specific inflammatory sinonasal disease patterns, the SSCT could serve as a more specific guide for FESS and allow a tailored endoscopic surgical technique.

A knowledge of the anatomy of the lateral wall of the nose and routes of mucociliary drainage of the paranasal sinuses is critical to understanding patterns of inflammatory sinonasal disease (Figs. 1 and 2). One of the major areas of mucociliary drainage is the region of the middle meatus, known as the ostiomeatal unit (OMU) (3, 10–14, 19–22). The other main region of sinus mucociliary drainage is the region of the sphenoethmoidal recess (SER) (Figs. 1 and 2). Coronal SSCT has been devised to optimally display the intricate anatomy of the OMU, SER, and paranasal sinuses (23). Previous reports of SSCT effectiveness have not distinguished specific patterns of inflammatory disease. In this report, we seek to establish the usefulness of designating radiologic patterns of inflammatory sinonasal disease as a more definitive guide to our surgical colleagues.

Materials and Methods

Over a 12-month period, SSCT scans were performed on 500 consecutive patients who were being evaluated for suspected inflammatory sinonasal disease and were under consideration for possible FESS. Each of the scans was performed with a GE 9800 quick CT scanner (General Electric, Milwaukee, WI) using a standard direct coronal technique. Patient preparation and scanning techniques were optimized to allow evaluation of the nonreversible component of the patients disease (ie, that component requiring FESS) and to insure excellent anatomic assess-
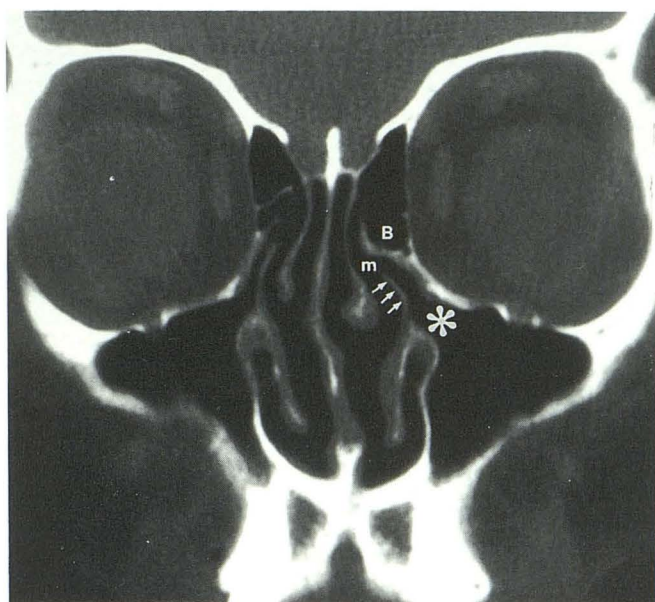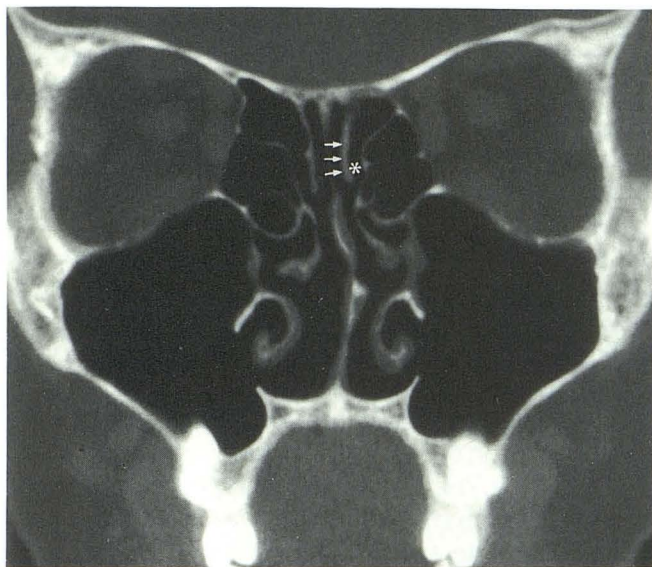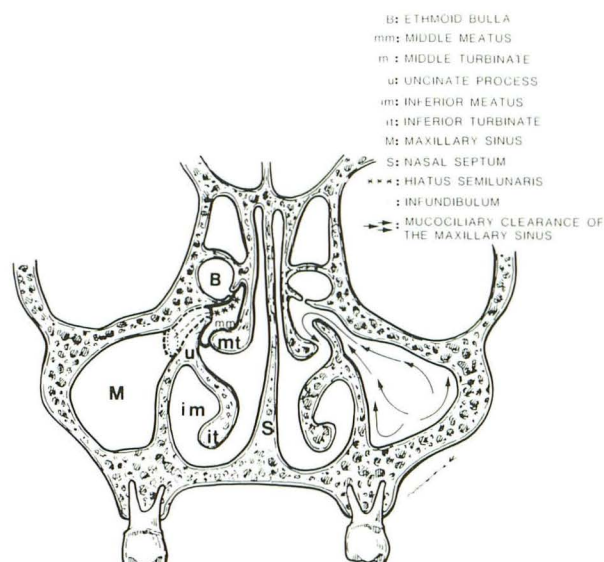
Fig. 2. *A*, Normal coronal SSCT example through OMU region demonstrating maxillary ostium (*asterisk*) leading into infundibulum, uncinate process (*arrows*), ethmoid bulla (*B*) and middle meatus (*m*).

B, Coronal plane cross-sectional line drawing through region of OMU depicting components of OMU on left side of drawing. Coronal view is excellent for delineating site of obstruction as seen in *infundibular pattern* (*heavy dashed line*) and *ostiomeatal unit pattern* (*solid line*). Right side of line drawing, maxillary sinus route of mucociliary clearance is depicted.

C, Normal coronal SSCT example at level of superior meatus. Sphenoid sinus ostium drains posterior to superior turbinate (*arrows*), while posterior ethmoid sinuses drain into superior meatus (*asterisk*). Patient has had bilateral medial antral window surgery.

ment of the major mucociliary drainage routes (23) (Table 1).

During evaluation of prior SSCT scans, recurring patterns of inflammatory disease were noted. Specifically, disease within the anterior sinuses that drain via the OMU or disease within the posterior sinuses that drain via the SER were distinguishable. Additionally, a high percentage of scans had demonstrated disease limited to the maxillary sinus, while others revealed limited disease without obvious OMU or SER involvement. Patients with sinonasal polyposis had been observed to have more diffuse disease. This led us to define five patterns of inflammatory disease: 1) limited maxillary sinus disease. 2) diffuse anterior disease, 3) posterior sinus disease, 4) sinonasal polyposis, and 5) limited disease without OMU or SER involvement. The CT scans of the 500 patients comprising the study group were

prospectively reviewed to confirm these recurring CT patterns of sinonasal disease and to delineate their frequency. Typical radiologic features of each pattern were ascertained and the relationship of the patterns to the known mucociliary drainage routes was assessed. Where possible, specific causal factors were delineated, including anatomical variants. Any noninflammatory disease processes were also noted.

Results

Patient demographic data included a male to female ratio of 227:273. The age range of the 500 patients was 4 to 86 years. Review of the CT scans on the 500 patients comprising the study
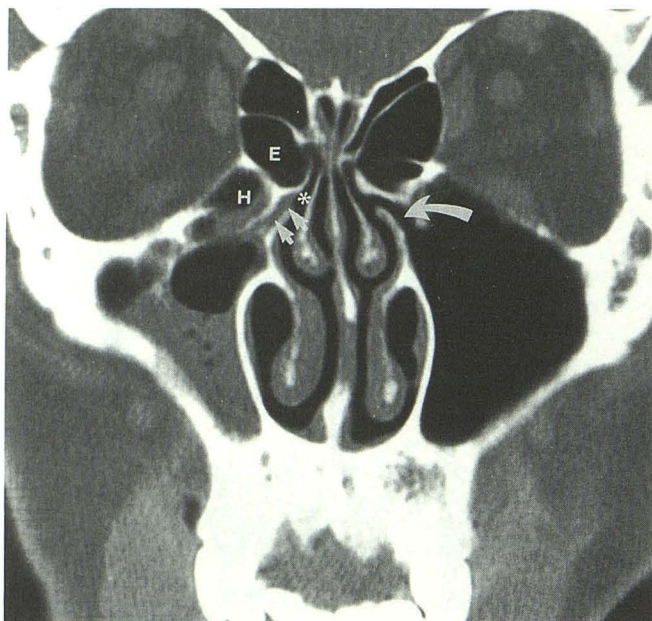
Fig. 3. Coronal SSCT example of *infundibular pattern* (pattern I) due to diseased right Haller cell (*H*) resulting in mucosal thickening within infundibulum (*arrows*) and leading to acute right maxillary sinusitis with air-fluid level. Ethmoid sinuses (*E*) are spared, as middle meatus (*asterisk*) remains patent. Left, unopacified infundibulum (*curved arrow*) is visualized.

population revealed normal SSCT scans in 133. In the remaining patients, inflammatory changes within the paranasal sinuses could be grouped into the five recurring patterns of inflammatory sinonasal disease that had been defined. Three of these patterns correlated with occlusion of known mucociliary drainage routes of the paranasal sinuses. These three distinctive obstructive patterns were designated the *infundibular* (*I*), *ostiomeatal unit* (*II*), and *sphenoethmoidal recess* (*III*) patterns. The infundibular pattern (I) was assigned for isolated maxillary sinusitis due to ipsilateral obstruction of the infundibulum (Fig. 3). The ostiomeatal unit pattern (II) was designated when the ipsilateral middle meatus was opacified resulting in sinusitis within some or all of the ipsilateral frontal, maxillary, and anterior and middle ethmoid sinuses (Fig. 4). The designation sphenoethmoidal recess pattern (III) was applied when obstruction was present posteriorly within the region of the SER, resulting in sphenoid and posterior ethmoid sinusitis (Fig. 5).

The two additional recurring patterns of inflammatory sinonasal disease that were designated included the *sinonasal polyposis pattern* (*IV*), diagnosed when a combination of polypoid softtissue densities were present throughout the nasal

cavity and paranasal sinuses in association with variable diffuse sinus opacification (Fig. 6). Typically, scans in these patients revealed variable infundibular enlargement and attenuation of the nasal septum and ethmoid bony trabeculae. Clinically, these patients were noted to have diffuse nasal polyposis. Air-fluid levels were also identified in 43% of patients with polyposis. The final designation was the *sporadic or unclassifiable pattern* (*V*). This pattern was specified for cases that did not fit into the obstructive patterns, I–III, and did not demonstrate evidence of polyposis. Within this classification were sporadic inflammatory sinus findings, including retention cysts, mucoceles, and mild mucoperiosteal thickening without coexistent OMU or SER obstruction (Fig. 7). Also included in this pattern were SSCT scans demonstrating postoperative changes.

The infundibular pattern was seen in 129 (26%) of the scans. The ostiomeatal unit pattern was identified in 126 (25%), with 32 (6%) scans demonstrating the sphenoethmoidal recess pattern. Sinonasal polyposis was present in 49 (10%) of the scans and in 121 (24%) the sporadic or unclassifiable pattern was designated. Normal scans were present in 133 (27%) of the 500. The total of all percentages is greater than 100, due to simultaneous occurrence of more than one pattern in some patients. Correlation of the endoscopic findings with the SSCT scan reports was excellent and will be the topic of future correspondence.

An important incidental finding was visualization of tumor or tumor-like condition in 26 scans (5%). Of the 26 noninflammatory lesions, 17 were benign osteomas (10 frontal, seven ethmoidal). The other nine suspicious lesions (2%) that were incidentally discovered included two antrochoanal polyps and, one each, fibrous dysplasia, nasal lymphoma, juvenile nasopharyngeal angiofibroma, giant nasal polyp, nasal angiomatous polyp, nasal melanoma, and Wegener granulomatosis. These nine cases, in addition to two complicated inflammatory cases (one OMU pattern with orbital abscess and one frontal pyomucocele), required extended sinonasal CT scans (intravenous iodinated contrast with imaging in both the axial and coronal planes) for full characterization of the lesions.

Additional incidental sinonasal CT abnormalities were noted. These included a variable amount of septal deviation identified in 200 patients (40%), septal spurs recognized in 76 scans (15%), synechiae, or intranasal adhesions, identified in
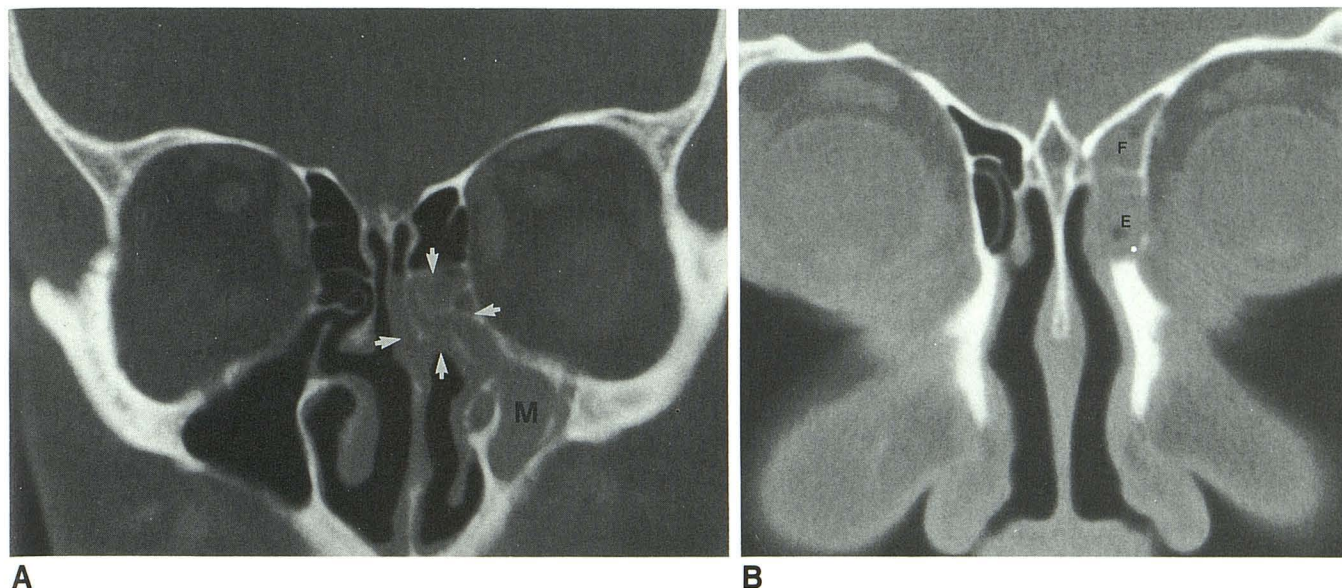
A **B**

Fig. 4. Coronal SSCT example of left *ostiomeatal unit pattern* (pattern II). *A*, Through region of OMU and *B*, more anteriorly through frontal sinus. Opacified OMU (*arrows*) has led to sinusitis within ethmoid (*E*), maxillary (*M*), and frontal (*F*) sinuses, typical of ostiomeatal unit pattern. Specific causal factor is not identified.

79 scans (16%), and concha bullosa that was present in 70 cases (14%), 28 of which were diseased.

Discussion

Direct coronal SSCT imaging results in exquisite delineation of sinonasal anatomy and pathology with images displayed in the same anatomic plane that is apparent during endoscopic surgery. Coupled with its noninvasive nature, these features have resulted in SSCT becoming the premier method for presurgical evaluation of patients with suspected inflammatory disease of the paranasal sinuses (12, 14, 15, 23). By optimizing the SSCT, a detailed presurgical map of the sinonasal region is rendered (23) (Fig. 8).

In our series, recurring patterns of sinonasal pathology were identified on SSCT, and endoscopic surgery was allowed to be tailored to that specific pattern of disease. Use of these patterns in the radiologic interpretation of SSCT scans results in grouping of patients into nonsurgical (normal CT), routine surgical (patterns I and II), and complex surgical (patterns III and IV) groups. The three obstructive patterns are responsible for the majority of inflammatory sinus disease and were identified in 57% of the 500 cases in our series. Radiologically, the polyposis pattern (IV) is composed of a consistent set of diagnostic CT observations that correlates with FESS findings. The sporadic pattern (V) was defined to encom-

pass cases that did not fall into the more well-defined groups I–IV.

The obstructive patterns (I–III) are understandable based upon the known major routes of mucociliary drainage that have been described (24, 25). Anteriorly, along the lateral wall of the nose, the middle meatus receives mucus from the frontal, maxillary, and anterior and middle ethmoid sinuses in the region designated as the OMU. Key components of the OMU include the maxillary ostium, the infundibulum, the uncinate process, the ethmoid bulla, and the hiatus semilunaris (Figs. 1 and 2). More posteriorly, the SER region drains the posterior ethmoid and sphenoid sinuses (Figs. 1 and 2). The sphenoid sinus drains posterior to the superior turbinate, directly into the SER, while the posterior ethmoid air cells drain into the posterior aspect of the superior meatus and then into the SER (Fig. 1). Pathology within the areas of mucociliary drainage accounts for the three obstructive patterns seen on SSCT (patterns I–III).

Pattern I: The Infundibular Pattern

The infundibular pattern, the most limited of the obstructive patterns, is diagnosed on SSCT when there is disease limited to the maxillary sinus with obstruction visualized within the ipsilateral ostium and infundibulum. The remainder of the OMU is patent, and consequently, the ipsilateral anterior and middle ethmoid, and fron-
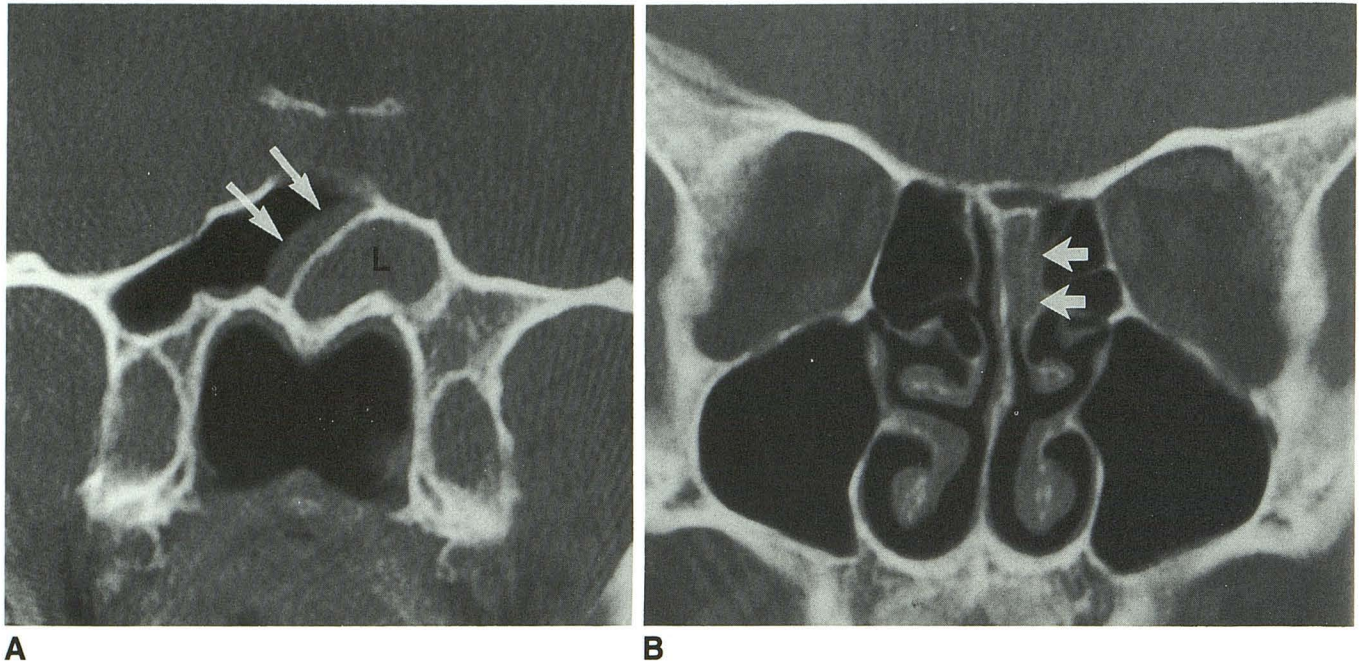
A   **B**

Fig. 5. *Sphenoethmoidal recess pattern* (pattern III) demonstrated on coronal SSCT scan.

A, Posterior image through sphenoid sinuses shows left sphenoid opacification (*L*) and secondary reactive mucosal thickening on right aspect of sphenoid sinus septum (*large arrows*).

B, Scan, more anterior, elucidates cause of sphenoid sinusitis, mucosal thickening within region of SER (*small arrows*).
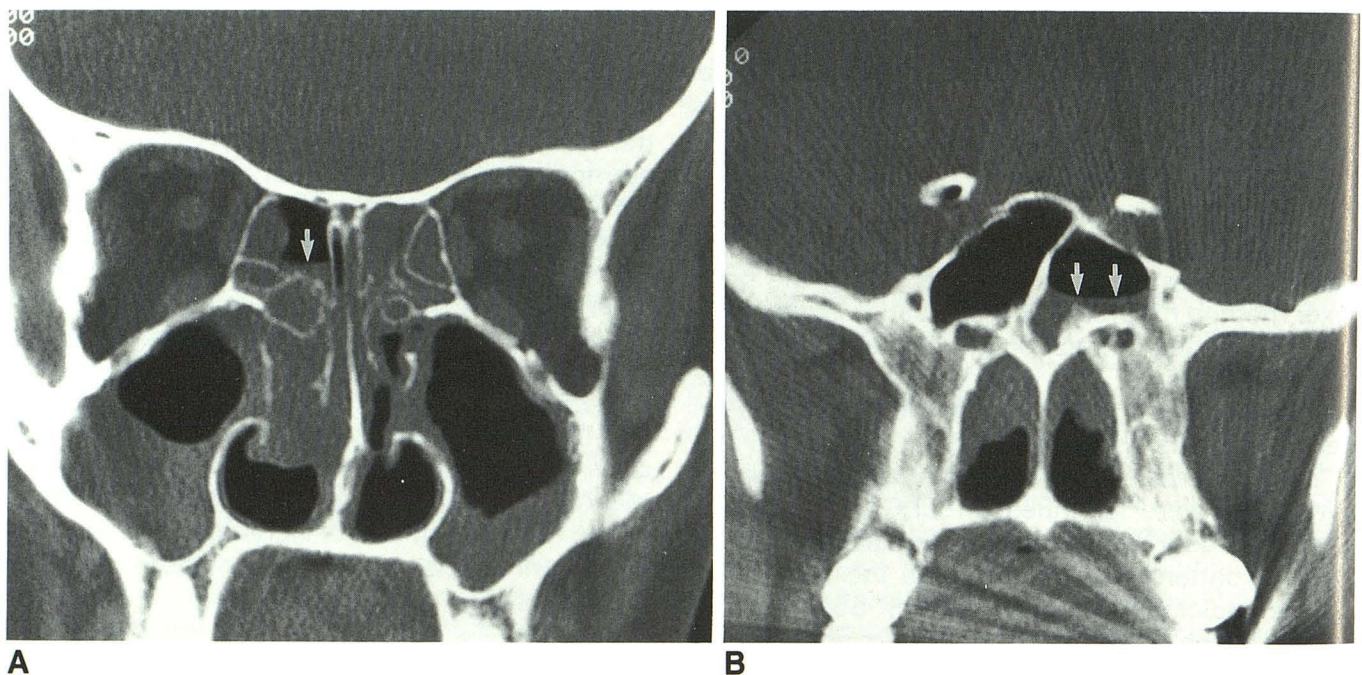

A   **B**

Fig. 6. Coronal SSCT scans, *A*, anterior through maxillary and ethmoid sinuses, *B*, posterior through sphenoid sinus, in patient with *sinonasal polyposis pattern* (pattern IV). Diagnostic radiologic features include prominent polypoid masses seen diffusely within nasal vault and paranasal sinuses with associated pansinus disease. Air-fluid levels (*arrows*) are commonly seen in addition to infundibular enlargement, bulging ethmoid sinus walls, and ethmoid trabeculae attenuation.

tal sinuses are normal. If there is any disease within the ipsilateral ethmoid bulla, this pattern is not diagnosed, rather the ostiomeatal unit pattern is described. Therefore, the infundibular pattern is designated when obstructive disease is limited to that component of the OMU that drains the
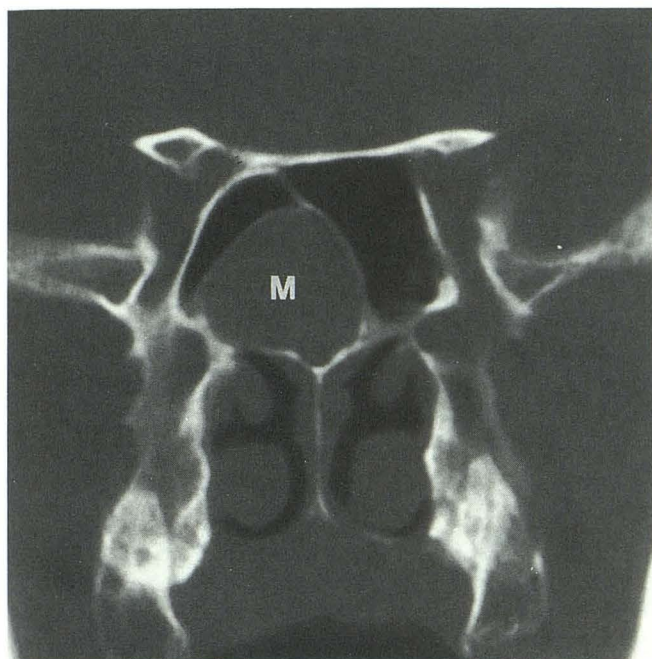
Fig. 7. Posterior image from SSCT demonstrating *sporadic pattern* (pattern V) of inflammatory sinonasal disease. An isolated sphenoid sinus mucocele (*M*) is present in this septated right sphenoid sinus. Remainder of scan, including OMU and SER regions, were normal.

maxillary sinus, the infundibulum. Since the anterior ethmoid and frontal sinuses may also drain via the infundibulum, it is presumed that in this pattern only the posteroinferior aspect of the infundibulum, that component into which the maxillary sinus ostia drains, is occluded.

Common visualized lesions of the infundibulum leading to the infundibular pattern include polyps, mucosal swelling, and anatomic variants, such as Haller cells that encroach upon and narrow the infundibulum. Hypoplastic maxillary sinuses are common and are associated with a long, attenuated infundibulum and consequently, are frequently responsible for an isolated infundibular pattern (10) (Fig. 9). When an isolated infundibular pattern is diagnosed on SSCT, endoscopic surgery can be limited to correction of the infundibular obstruction. This pattern requires the least amount of surgical intervention, and the anticipated surgical result is excellent. Often infundibulotomy alone will correct the problem (17). Surgical complications and disease recurrence are rare (26).

Pattern II: The Ostiomeatal Unit Pattern

Most descriptions of inflammatory sinonasal disease emphasize the ostiomeatal unit pattern

(3, 4, 6, 12, 14). When complete, the ostiomeatal unit pattern leads to inflammatory involvement within the ipsilateral maxillary, frontal, and anterior and middle ethmoid sinuses. Occlusion of the middle meatus, the common area of drainage for each of these sinuses, is responsible for this pattern of inflammatory sinus disease. The pattern may be incomplete due to a variable amount of disease involvement within the middle meatus and OMU components, and due to variable placement of the draining ostia. This latter point has been specifically noted for the nasofrontal duct that drains the frontal sinus (21). The nasofrontal duct can end at variable locations within the middle meatus. If the duct is more anteriorly located, the frontal sinus may be spared from inflammatory disease in the ostiomeatal pattern. Isolated frontal sinus disease could occur when the obstructive lesion is limited to the anterior aspect of the middle meatus. In our experience, this is rare.

Diagnosis of the ostiomeatal unit pattern on SSCT is made when the CT images demonstrate opacification of the middle meatus with ipsilateral inflammatory changes within some or all of the anterior and middle ethmoid, maxillary, and frontal sinuses. When an OMU pattern of sinus opacification is observed on SSCT, then specific attention should be directed to the components of the OMU/middle meatus region. An attempt should be made to define possible causes of opacification within the OMU. Common causes of OMU obstruction include mucosal swelling, hypertrophied turbinates, polyps, adhesions, nasal tumors, and anatomic variants such as concha bullosa, paradoxical middle turbinates, and septal deviation with or without spur (10) (Figs. 4 and 8).

The surgical approach to the OMU pattern is more extensive than with the infundibular pattern due to the involvement of multiple ostia within the middle meatus (4, 6). The identification of this pattern on SSCT allows a tailored surgical plan that usually includes infundibulotomy in combination with ethmoid bullectomy and, at times, more extensive ethmoidectomy. Any identified causal lesions are also surgically corrected. Due to the more extensive surgical therapy required, the complication and failure rates are greater than with intervention for the infundibular pattern. However, excellent surgical results are still anticipated (26).
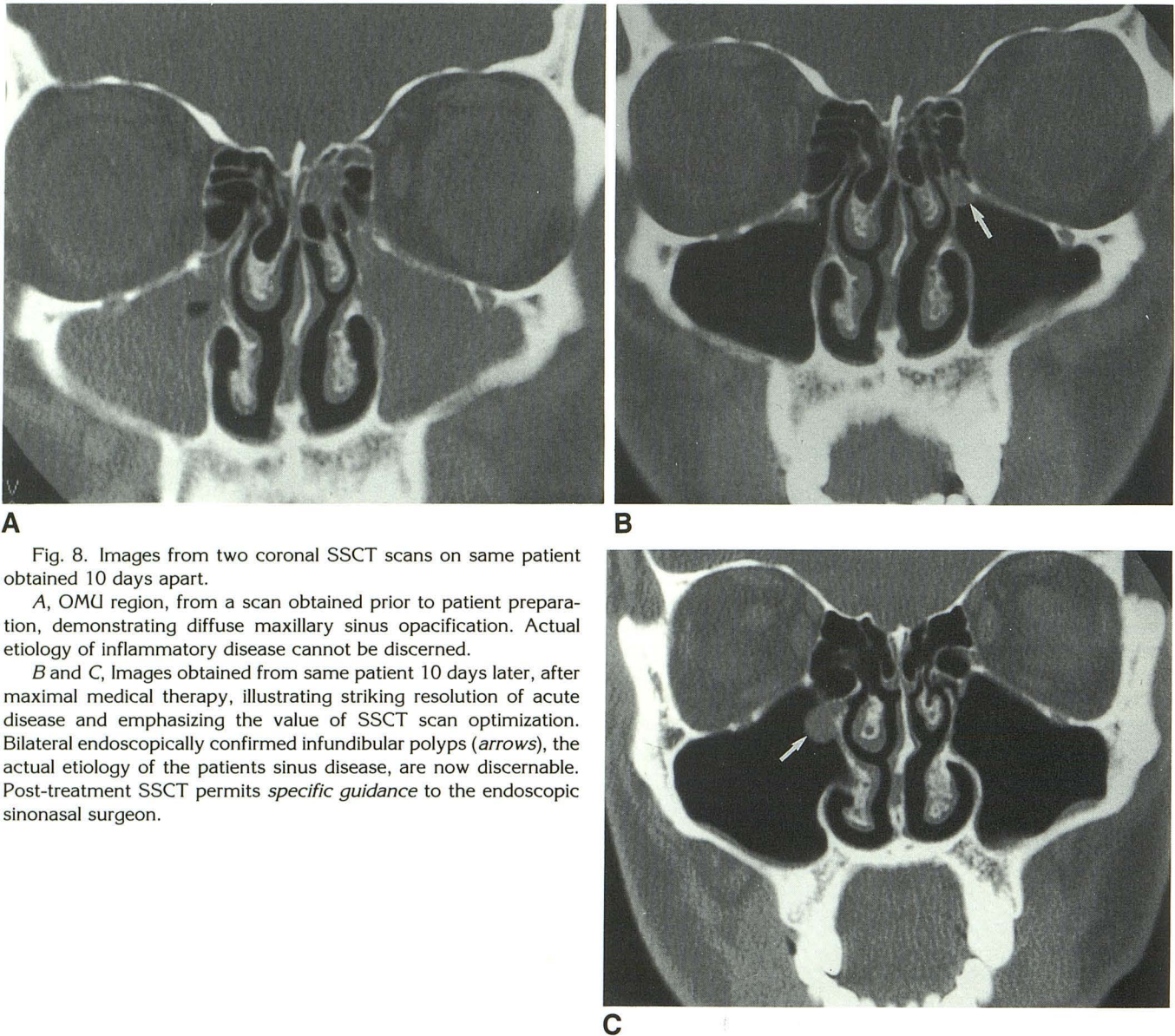
A

B

Fig. 8. Images from two coronal SSCT scans on same patient obtained 10 days apart.

A, OMU region, from a scan obtained prior to patient preparation, demonstrating diffuse maxillary sinus opacification. Actual etiology of inflammatory disease cannot be discerned.

B and *C,* Images obtained from same patient 10 days later, after maximal medical therapy, illustrating striking resolution of acute disease and emphasizing the value of SSCT scan optimization. Bilateral endoscopically confirmed infundibular polyps (*arrows*), the actual etiology of the patients sinus disease, are now discernable. Post-treatment SSCT permits *specific guidance* to the endoscopic sinonasal surgeon.

C

Pattern III: The Sphenoethmoidal Recess Pattern

When pathology leads to obstruction of sinus ostia posteriorly, in the area of the SER, the ipsilateral posterior ethmoid and sphenoid sinuses are variably involved with inflammatory changes. This is the sphenoethmoidal recess pattern and is readily apparent on SSCT due to the typical inflammatory disease within the sphenoid sinus and, to a lesser extent, within the posterior ethmoid sinuses. When this pattern is identified, associated opacification of the SER can usually be visualized (Fig. 5). Isolated sphenoid disease, without posterior ethmoid sinus disease, can be seen in the SER pattern since the sphenoid sinus drains directly into the SER, whereas the posterior

ethmoid initially drains more anteriorly into the superior meatus.

The posteriorly located SER is understandably more difficult to reach at endoscopy, and surgery to correct pathologic processes causing this pattern is more challenging. There is also an expected increased surgical complication rate compared to the other obstructive patterns (4, 6, 7).

The other two radiologic patterns of inflammatory sinus diseases identifiable on SSCT are the sinonasal polyposis pattern (IV) and the sporadic or unclassifiable pattern (V). These patterns are not the direct result of mucociliary drainage obstruction. It is important to recognize and identify these patterns, as the therapy and extent of FESS is significantly different than with the ob-
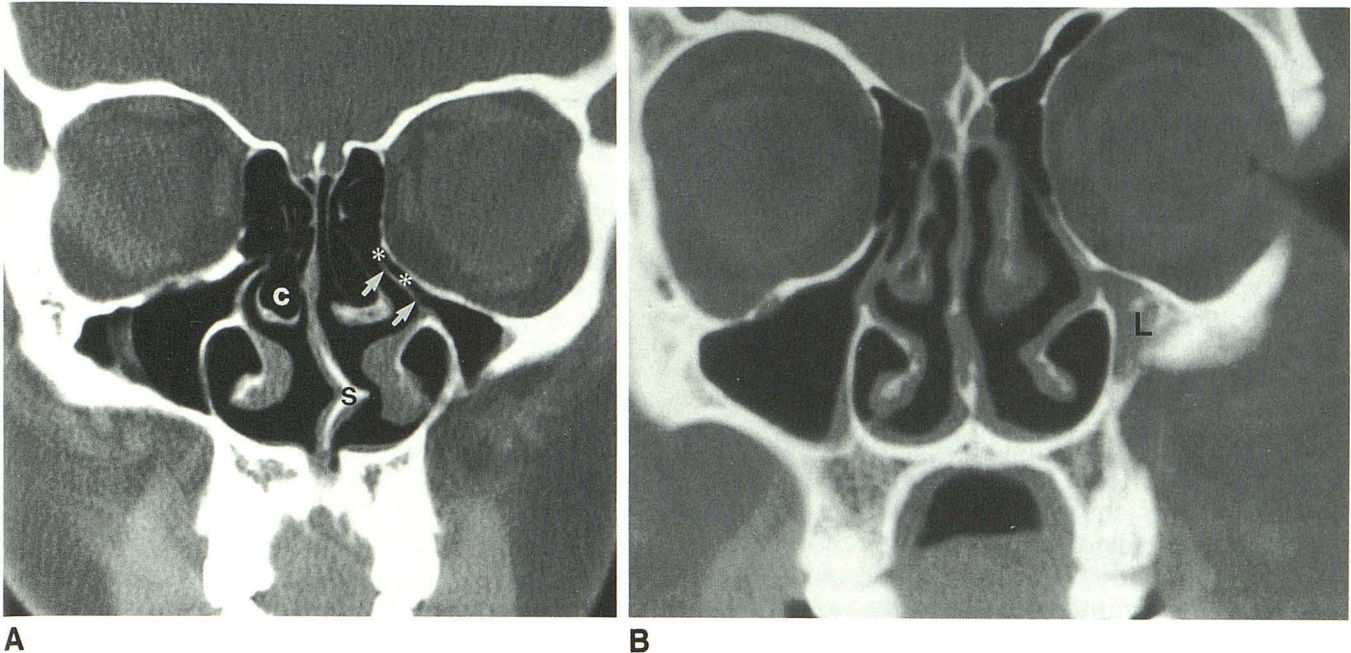
A   B

Fig. 9. A, Nondiseased and B, diseased examples of hypoplastic maxillary sinuses (different patients). In image A note elongated uncinate process (arrows) with narrowed infundibulum (asterisks) on left, typical of maxillary sinus hypoplasia. Also note incidental bilateral concha bullosa (C) and septal deviation with spur (S). Image B demonstrates the more typical diseased hypoplastic maxillary sinus with opacification (L). Long narrowed infundibulum is predisposed to easy obstruction leading to infundibular pattern of inflammatory sinus disease.

structive patterns. The preoperative radiologic diagnosis of these patterns is extremely helpful to the endoscopic surgeon.

Pattern IV: The Sinonasal Polyposis Pattern

Distinct, characteristic, radiologic findings are present on SSCT in patients with sinonasal polyposis (27). In this disease process, polyps are diffusely present within the nasal cavity and paranasal sinuses. Characteristic SSCT findings that are variably present include polypoid masses filling the nasal vault and sinuses, bilateral infundibular enlargement, convex (bulging) ethmoid sinus walls, and attenuation of the bony nasal septum and ethmoid trabeculae. Because the polyps may occlude the mucociliary drainage routes, a mixture of inflammatory patterns I-III may be present. Air-fluid levels are frequent but do not always indicate acute sinusitis, as normal secretions may accumulate without infection. Correlation for clinical evidence of acute sinusitis is necessary in these circumstances. The label sinonasal polyposis is reserved for diffuse polyposis. Isolated polyps are not included but categorized by the pattern of sinusitis that results from the obstructing polyp (Fig. 8).

Sinonasal polyposis is frequently treated medically with chronic adrenocortical steroids and with antibiotic therapy for acute bouts of sinusitis (28). Surgical intervention is utilized for medical therapy failure. The required endoscopic surgery is much more involved and difficult than in patterns I-III, due to the extensive pansinus polypoid disease and tendency for the recurring formation of polyps. Consequently, the surgical complication rate is increased and vigorous bleeding may be encountered. Reactive mucosa that is present in patients with sinonasal polyposis may lead to poorer long-term surgical results and the need for possible repeated surgeries (26).

Pattern V: Sporadic (Unclassifiable) Pattern

The sporadic pattern is diagnosed when inflammatory sinonasal disease is not attributable to obstruction of known mucous drainage routes or polyposis, but rather, there is randomly placed disease noted anywhere within the sinuses. This group includes individual inflammatory lesions such as retention cysts and mucoceles. Also included in this group are SSCT scans demonstrating postsurgical changes. SSCT findings are varied due to the variety of processes included in the sporadic pattern. The specific process that is present will dictate the actual CT findings. These range from isolated inflammatory changes within the sinuses in the absence of mucous drainage

route obstruction, to the more specific entities of retention cysts and mucoceles, as well as randomly located postsurgical changes.

Endoscopic surgical intervention in this group is tailored to the specific findings. Surgical outcomes varies, but is usually good. The degree of surgical difficulty and the chances of complications vary greatly in this group, depending on the lesion type and accessibility of the affected sinus.

An additional important observation in our series of SSCT scans was identification of tumor or tumor-like condition in 5% of the cases. The majority of these were incidental osteomas. However, in 2% of the total cases, an incidental significant lesion was identified, necessitating a full sinus CT for characterization. When atypical inflammatory findings are noted on SSCT scans or in patients with unusual histories, additional imaging is warranted to exclude significant noninflammatory (tumor) or complicated inflammatory lesions (osteomyelitis, intracranial involvement, etc) (10, 14, 23).

In conclusion, we have characterized inflammatory sinonasal disease into five distinct radiologic patterns, each with a different therapeutic course and surgical options. A more precise interpretation of SSCT scans is rendered when inflammatory sinonasal disease is categorized into these distinct radiologic patterns. When a specific obstructive pattern is identified, detailed attention can be directed to the likely site of obstruction with possible definition of a specific etiology. A detailed road map of relevant surgical anatomy and pathology is then available for the endoscopic surgeon. It is anticipated that this will result in more directed and specific functional endoscopic sinonasal surgery with improved patient care and surgical result.

References

1. Levine HL. Functional endoscopic sinus surgery: evaluation, surgery, and follow-up of 250 patients. *Laryngoscope* 1990;100:79–84
2. Rice DH. Endoscopic sinus surgery: results at 2-year followup. *Otolaryngol Head Neck Surg* 1989;10:476–479
3. Kennedy DW, Zinreich SJ, Rosenbaum AE, et al. Functional endoscopic sinus surgery: theory and diagnostic evaluation. *Arch Otolaryngol* 1985;111:576–582
4. Kennedy DW. Functional endoscopic sinus surgery: technique. *Arch Otolaryngol* 1985;111:643–649
5. Kamel R. Endoscopic transnasal surgery in antrochoanal polyp. *Arch Otolaryngol Head Neck Surg* 1990;116:841–843
6. Rice DH. Basic surgical techniques and variations of endoscopic sinus surgery. *Otolaryngol Clin North Am* 1989;22:713–725
7. Schaefer SD. Endoscopic total sphenoethmoidectomy. *Otolaryngol Clin North Am* 1989;22:727–732
8. Stammberger H. Endoscopic endonasal surgery: concepts in treatment of recurring rhinosinusitis. I. Anatomic and pathophysiologic considerations. *Otolaryngol Head Neck Surg* 1986;94:143–146
9. Stammberger H. Endoscopic endonasal surgery: concepts in treatment of recurring rhinosinusitis. II. Surgical technique. *Otolaryngol Head Neck Surg* 1986;94:147–156
10. Harnsberger HR. The sinuses and nose. In: Harnsberger HR, ed. *Handbooks in radiology, head and neck imaging.* Chicago, Year Book, 1990:377–419
11. McAlister WH, Lusk R, Muntz HR. Comaprison of plain radiographs and coronal CT scans in infants and children with recurrent sinusitis. *AJR* 1989;153:1259–1264
12. Zinreich SJ, Kennedy DW, Rosenbaum AE, et al. Paranasal sinuses: CT imaging requirements for endoscopic surgery. *Radiology* 1987;163:769–775
13. Schatz CJ, Becker TS. Normal CT anatomy of the paranasal sinuses. *Radiol Clin North Am* 1984;22:107–118
14. Pollei SR, Harnsberger HR. The radiologic evaluation of the sinonasal region. *Postgrad Radiol* 1989;9:242–264
15. Chow JM, Mafee MF. Radiologic assessment preoperative to endoscopic sinus surgery. *Otolaryngol Clin North Am* 1989;22:691–701
16. Messerklinger W. On the drainage of the normal frontal sinus of man. *Acta Otolaryngol* 1967;673:176–181
17. Drettner B. The obstructed maxillary ostium. *Rhinology* 1967;51:100–104
18. Proctor DF. The mucociliary system. In: Proctor DF, Andersen IHP, eds. *The nose: upper airway physiology and the atmospheric environment.* New York: Elsevier, 1982
19. Becker SP. Anatomy for endoscopic sinus surgery. *Otolaryngol Clin North Am* 1989;22:677–682
20. Calhoun KH, Rotzler WH, Stiernberg CM. Surgical anatomy of the lateral nasal wall. *Otolaryngol Head Neck Surg* 1990;102:156–160
21. Wallace R, Salazar JE, Cowles S. The relationship between frontal sinus drainage and osteomeatal complex disease: a CT study in 217 patients. *AJNR* 1990;11:183–186
22. Som PM. CT of the paranasal sinuses. *Neuroradiology* 1985;27:189–201
23. Babbel RW, Harnsberger HR, Nelson B, et al. Optimization of techniques in screening CT of the sinuses. *AJNR* 1991;12:849–854
24. Proctor DF. The nose, paranasal sinuses and pharynx. In: Walters W, ed. *Lewis-Walters practice of surgery.* Hagerstown, MD: Little Brown, 1982;4:1–37
25. Drettner B. The paranasal sinuses. In: Proctor DF, Anderson IHP, eds. *The nose: upper airway physiology and the atmospheric environment.* New York: Elsevier, 1982
26. Stankiewicz JA. Complications of endoscopic sinus surgery. *Otolaryngol Clin North Am* 1989;22:749–758
27. Som PM, Sacher M, Lawson W, et al. CT appearance distinguishing benign nasal polyps from malignancies. *J Comput Assist Tomogr* 1987;11:129–133
28. Josephson JS. The role of endoscopic sinus surgery for the treatment of nasal polyposis. *Otolaryngol Clin North Am* 1989;22:831–840